Magnetic flux noise in the three-Josephson-junction superconducting ring

E. Il'ichev

Institute of Photonic Technology, 9 Albert-Einstein Str., 07745, Jena, Germany

A. N. Omelyanchouk[a)]

B. Verkin Institute for Low Temperature Physics and Engineering of the National Academy of Sciences of Ukraine, 47 Lenin Ave., Kharkov 61103, Ukraine

(Submitted January 11, 2008)
Fiz. Nizk. Temp. **34**, 520–524 (June 2008)

We analyze the influence of noise on magnetic properties of a superconducting loop which contains three Josephson junctions. This circuit is a classical analog of a persistent current (flux) qubit. A loop supercurrent induced by external magnetic field in the presence of thermal fluctuations is calculated. To connect with experiment, we calculate the impedance of a low-frequency tank circuit which is inductively coupled with the loop of interest. We compare the results with the results obtained in the quantum mode — when the three junction loop exhibits quantum tunneling of the magnetic flux. We demonstrate that the tank–loop impedance in the classical and quantum modes have different temperature dependence and can be easily distinguished experimentally. © *2008 American Institute of Physics*. [DOI: 10.1063/1.2920076]

I. INTRODUCTION

Magnetic flux quantization in superconductors is used, in particular, for realization of very sensitive magnetometers. One of them is so-called radio-frequency (rf) SQUID.[1] The sensor of rf SQUIDs is a single junction interferometer — a Josephson junction which is incorporated in a superconducting ring with a sufficiently small inductance L. When an external flux Φ_e is applied to an interferometer loop, the circulating supercurrent I is induced and a flux Φ_i is admitted into the ring:

$$\Phi_i = \Phi_e - IL. \tag{1}$$

The phase difference φ across a Josephson junction equals the normalized magnetic flux in the interferometer loop:

$$\varphi = 2\pi\frac{\Phi_i}{\Phi_0} + 2\pi n, \tag{2}$$

where Φ_0 is the flux quantum, and n is an integer. Since the Josephson current is related to the phase difference φ:

$$I = I_c \sin\varphi, \tag{3}$$

where I_c is the critical current, Eq. (1) can be rewritten:

$$\varphi = \varphi_e - \beta\sin\varphi \tag{4}$$

where $\varphi_e = 2\pi\Phi_e/\Phi_0$ is the normalized external flux, and the constant

$$\beta = 2\pi LI_c/\Phi_0 \tag{5}$$

is the normalized inductance of the interferometer.

From Eq. (4) it is clearly seen that the magnetic properties of a single junction interferometer are defined by the parameter β. If $\beta<1$ the $\varphi_e(\varphi)$ dependence is unique (see Fig. 1), and the corresponding mode of SQUID operation is called nonhysteretic. If $\beta>1$ the $\varphi_e(\varphi)$ dependence is multivalued (see Fig. 1), and corresponding mode of SQUID operation is hysteretic.

An rf SQUID basically consists of a sensor (usually a single junction interferometer) inductively coupled to a radio-frequency-biased tank circuit. The flux φ_e applied to the sensor changes the effective inductance (or/and the effective resistance) of the tank–sensor arrangement. Thus, a flux change can be detected as changes in phase (or/and amplitude) of the voltage across the tank circuit.

The classical mode for the single junction interferometer as well as for corresponding rf SQUID in the presence of fluctuations have been investigated in detail theoretically as well as experimentally.[2–7] On the other hand the quantum mode for this device is difficult to realize. Since the interferometer should be hysteretic, it requires a finite LI_c product and therefore a finite coupling with the environment. In order to avoid this problem, substitution of the geometrical inductance by a Josephson one has been proposed. Indeed, if the number of Josephson junctions in the loop $m>2$ and for suitable junctions parameters, a doubly degenerate state exists at any geometrical inductance L. One of the simplest realizations here is a three-junction interferometer, which is called also a persistent current (or flux) qubit.[8] Such a qubit

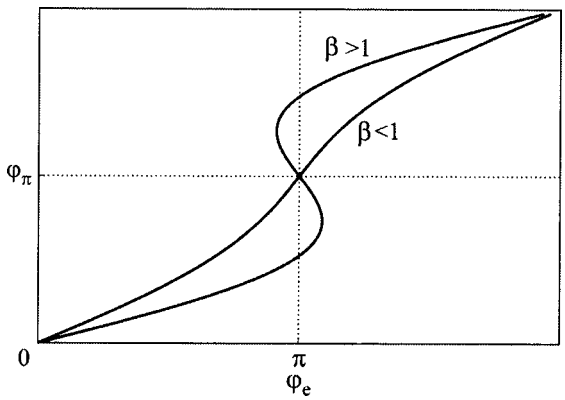

FIG. 1. $\varphi(\varphi_e)$ for rf SQUID in nonhysteretic and hysteretic modes.

has been fabricated by several teams, and the quantum regime was convincingly demonstrated.

If external magnetic flux is

$$\varphi = \pi + 2\pi n \tag{6}$$

the hysteretic interferometer exhibits doubly degenerate energy states; see Fig. 2. These states correspond to the different directions of the interferometer current. If temperature is low enough and for suitable parameters of Josephson junctions the magnetic flux can tunnel between the two potential minima. Below we will call the systems under consideration quantum if in their dynamics there is quantum tunneling. If, for some reasons, the quantum tunneling is suppressed, we will call these systems classical ones.

It is clear that the presence of quantum tunneling ensures the absence of hysteresis in the $\varphi(\varphi_e)$ dependence. On the other hand, jumps between two energy minima can be originated by fluctuations, and the hysteresis will be washed out. Therefore, for both cases considered above, the mode of the rf SQUID operation will be nonhysteretic. A natural question arises: By analyzing a SQUID output signal is it possible to distinguish between quantum mode (interferometer with "quantum leak") and classical mode (interferometer in the presence of fluctuations)? We address this paper to that question.

II. CLASSICAL MODE OF A FLUX QUBIT IN THE PRESENCE OF FLUCTUATIONS

The system studied presents a superconducting circuit (ring) with three Josephson junctions; see Fig. 3. We consider the case of small self-inductance of the ring $L \to 0$, and therefore $\Phi_e = \Phi_i$. The phases across each junction in the qubit loop φ_i satisfy

$$\varphi_1 + \varphi_2 + \varphi_3 = \varphi_e.$$

In the framework of the RSJ model for Josephson junctions the current through each junction is:

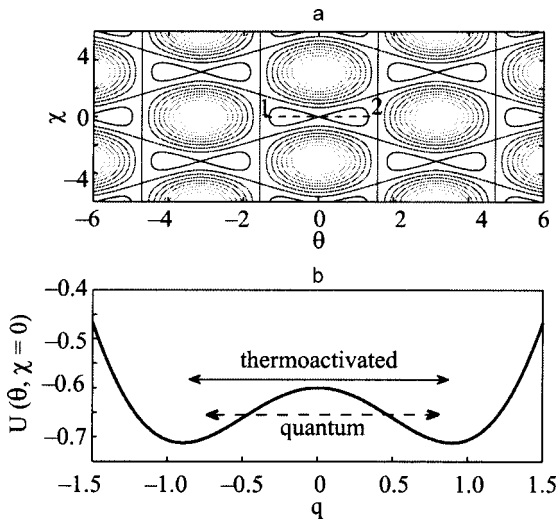

FIG. 2. Contour plot of the potential $U(\theta,\chi)$ (13), $\alpha=0.8$ (a). Bistable potential profile along line 1–2 in Fig. 2a at $\varphi_e=\pi$, $\alpha=0.8$ (b).

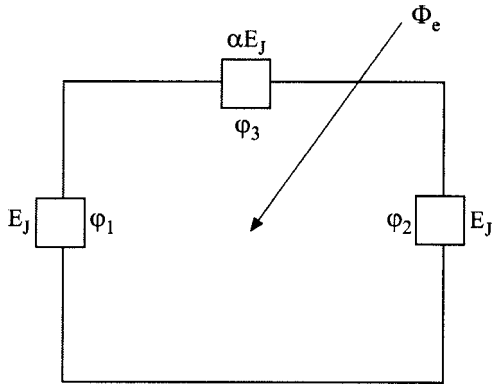

FIG. 3. Scheme of the persistent current (flux) qubit.

$$I = \frac{\hbar C_i}{2e}\frac{d^2}{dt^2}\varphi_i + \frac{\hbar}{2eR_i}\frac{d}{dt}\varphi_i + I_{ci}\sin\varphi_i + \delta I_i(t), \quad i = 1,2,3 \tag{7}$$

where $\hbar$ is Planck's constant, e is the electron charge, C_i and R_i are the junctions' capacitances and resistances, respectively. We restrict ourselves to a practical case, when two junctions in the loop are identical: $C_1=C_2=C$, $I_{c1}=I_{c2}=I_c$, $R_1=R_2=R$ and the third junction has slightly smaller critical current (with the same critical current density) $I_{c3}=\alpha I_c$, $0.5<\alpha<1$ and therefore $C_3=\alpha C$, $R_3=R/\alpha$. The presence of the "white noise" is given by the fluctuation currents $\delta I_i(t)$ with correlator $\langle \delta I_i(t)\delta I_i(t')\rangle = 2kT/R_i\delta(t-t')$ and mean value $\langle \delta I_i(t)\rangle = 0$.

In dimensionless units:

$$\omega_R = 2eRI_c/\hbar, \quad \omega_R t = \tau \tag{8}$$

and for negligible capacitance, Eq. (7) can be rewritten:

$$I/I_c = d\varphi_{1,2}/d\tau + \sin\varphi_{1,2} + \delta\varphi_{1,2} = \alpha d\varphi_3/d\tau + \alpha\sin\varphi_3 + \delta\varphi_3(\tau). \tag{9}$$

The correlators of $\delta\varphi_i$ are:

$$\langle \delta\varphi_i(\tau)\delta\varphi_i(\tau')\rangle = 2D\delta_i(\tau-\tau'), \tag{10}$$

where $D=kT/E_J$, $E_J=\hbar I_c/2e$.

By introducing the phases θ and χ

$$2\theta = \varphi_1 + \varphi_2, 2\chi = \varphi_1 - \varphi_2,$$

and taking into account that $\varphi_3=\varphi_e-2\theta$, Eq. (7) can be presented in the form:

$$d\chi/d\tau = -\cos\theta\sin\chi + 1/2(\delta\varphi_2 - \delta\varphi_1),$$

$$(1+2\alpha)d\theta/d\tau = -\sin\theta\cos\chi + \alpha\sin(\varphi_e - 2\theta) + \delta\varphi_3(\tau) - 1/2(\delta\varphi_2 + \delta\varphi_1).$$

These equations can be reduced to:

$$\frac{d\chi}{d\tau} = -\frac{\partial U}{\partial\chi} + \delta\chi(\tau), \tag{11}$$

$$\frac{d\theta}{d\tau} = -\frac{1}{(1+2\alpha)}\frac{\partial U}{\partial\theta} + \delta\theta(t). \tag{12}$$

where

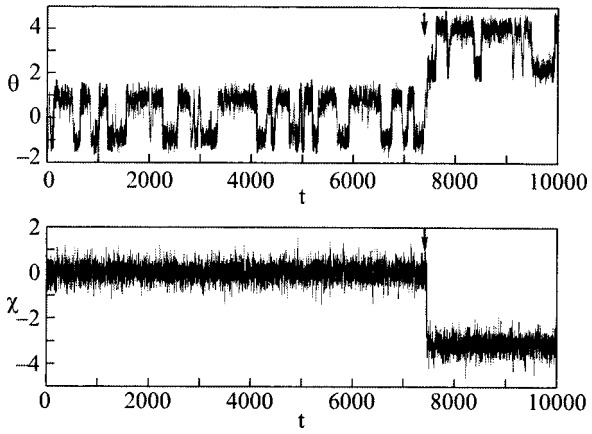

FIG. 4. The random motion of phases θ and χ in a bistable potential for $\varphi_e=\pi$, $\alpha=0.8$, and $D=0.1$.

$$U(\theta,\chi) = -\cos\theta\cos\chi - \frac{1}{2}\alpha\cos(\varphi_e - 2\theta) \tag{13}$$

is the effective potential and the random forces are:

$$\langle \delta\chi(\tau)\delta\chi(\tau')\rangle = D\delta(\tau-\tau'),$$

$$\langle \delta\theta(\tau)\delta\theta(\tau')\rangle = \frac{3}{(1+2\alpha)^2}D\delta(\tau-\tau').$$

The Langevin equations (11) and (12) describe the random motion of the "particle" with coordinates (θ,χ) in the periodic potential (13), which is a set of bistable cells (eight-shaped contours in Fig. 2a). We have numerically integrated these stochastic equations by Ito's method (see, e.g., Ref. 9) for different values of parameter α and the strength of the fluctuations D. Typical traces of $\theta(\tau)$ and $\chi(\tau)$ are shown in Fig. 4. They correspond to random motion in a bistable potential; Fig. 2. The arrows indicate the switching from one unit cell in Fig. 2a to another. With knowledge of $\theta(\tau)$ and $\chi(\tau)$ the average circulating current in the ring is obtained as:

$$I(\varphi_e) = I_c\langle\langle\sin(\chi+\theta)\rangle\rangle. \tag{14}$$

The averaging $\langle\langle\ldots\rangle\rangle$ includes, for each value of flux φ_e, an average over time of the traces $(\theta(\tau),\chi(\tau))$ and an average over a set of 50 traces.

The the current–flux curves calculated in such a way for different values of D and different values of the parameter α are presented in Figs. 5 and 6.

From Eqs. (11)–(13) one can reconstruct the Fokker–Planck equation for the distribution function $P(\chi,\theta)$:

$$\frac{\partial P}{\partial\tau} = \frac{\partial}{\partial\chi}\left(\frac{\partial U}{\partial\chi}P\right) + \frac{D}{2}\frac{\partial^2}{\partial\chi^2}P + \frac{1}{1+2\alpha}\frac{\partial}{\partial\theta}\left(\frac{\partial U}{\partial\theta}P\right) + \frac{1}{2}\frac{3D}{(1+2\alpha)^2}\frac{\partial^2}{\partial\theta^2}P. \tag{15}$$

The Fokker–Planck equation (15) admits a stationary potential solution (see Ref. 9) in the special case $\alpha=1$, i.e., when all three junctions are identical. For $\alpha=1$ the analytical solution reads:

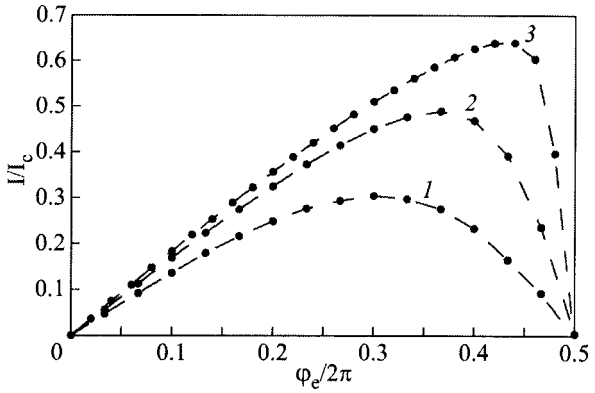

FIG. 5. The dependences $I(\varphi_e)$ for $\alpha=0.8$ and $D=0.5$ (*1*), $D=0.25$ (*2*), $D=0.1$ (*3*).

$$P = \frac{\exp\left(-\frac{2}{D}U(\chi,\theta)\right)}{N}, \tag{16}$$

$$N = \iint d\chi d\theta \exp\left(-\frac{2}{D}U(\chi,\theta)\right). \tag{17}$$

Since the potential U is a 2π-periodic function of the variables χ and θ, the average current in the ring is:

$$\frac{I}{I_c} = \frac{\int_0^{2\pi}\int_0^{2\pi} d\chi d\theta \sin(\chi+\theta)\exp\left(-\frac{2}{D}U(\chi,\theta)\right)}{\int_0^{2\pi}\int_0^{2\pi} d\chi d\theta \exp\left(-\frac{2}{D}U(\chi,\theta)\right)}. \tag{18}$$

In Fig. 7 we compare the numerical results (circles) and the $I(\varphi_e)$ obtained from the analitical formula (18) (solid line) for the case $\alpha=1$ and $D=0.2$. This comparison was used as an additional calibration of our numerical procedure, which works for arbitrary values of α.

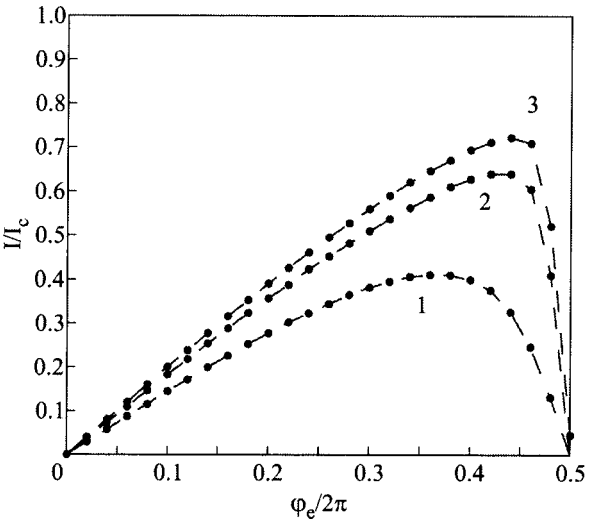

FIG. 6. The dependences $I(\varphi_e)$ for $D=0.1$ and $\alpha=0.5$ (*1*), $\alpha=0.8$ (*2*), $\alpha=1$ (*3*).

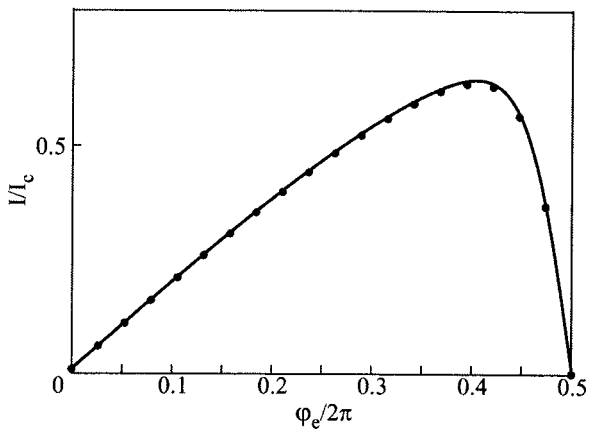

FIG. 7. Comparision of numerical (circles) and analytical (solid line) calculations. $D=0.2$, $\alpha=1$.

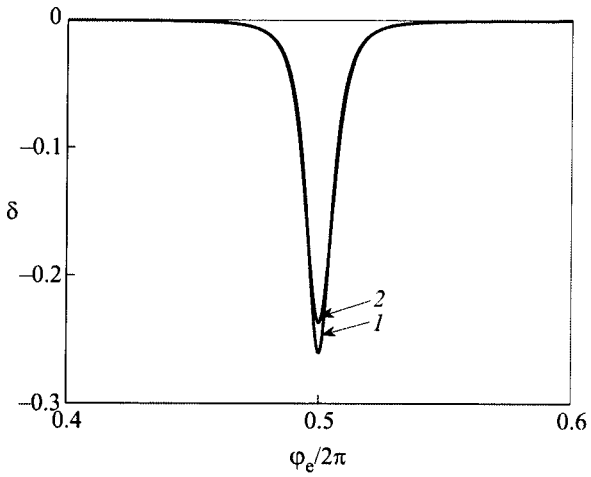

FIG. 9. The phase shift $\delta(\varphi_e)$ in the quantum mode. $T/\Delta=0.1$ (*1*), $T/\Delta=1$ (*2*).

III. THE PROBING OF QUBIT'S STATE IN CLASSICAL AND QUANTUM MODES

As we wrote in the Introduction, we probe a qubit with the use of a tank circuit by the impedance measurement technique.[10] It has been convincingly shown[10,11] that the observable phase difference $\delta(\varphi_e)$ between the tank current I_{rf} and tank voltage V_{rf} in both the classical and quantum modes reads:

$$\tan\delta(\varphi_e)\approx\Theta\frac{dI}{d\varphi_e}, \tag{19}$$

where Θ is a constant which characterizes the inductive coupling of the qubit with the tank circuit. Using the results of Sec. II, we calculated output signal $\delta(\varphi_e)$ for the classical noise-affected mode. For different levels of noise D (all of those correspond to the nonhysteretic regime) the $\delta(\varphi_e)$ curves are shown in Fig. 8.

In the quantum noise free mode (see Appendix A) the nonhysteretic behavior is achieved by the tunneling between two wells. The phase shift $\delta(\varphi_e)$ in this case is described by Eqs. (19), (A1). It is presented in Fig. 8 for the same values as in the classical case for the qubit–tank coupling constant Θ and experimentally realized qubit parameters $I_p\Phi_0=200$ GHz, $\Delta=1.5$ GHz.

Comparing the classical and quantum modes (Figs. 8 and 9), we have found that in quantum mode the dip on the $\delta(\varphi_e)$ curve remains constant over a wide temperature range $kT\leq\Delta$. This reflects the fact that tunneling splitting Δ does not depend on the temperature. The depth of the dip is changed with temperature — excitations to the upper level depress the value of the average qubit current. For the classical mode the situation is rather different. First of all, for a reasonable set of qubit parameters it is impossible to get such a narrow and profound dip as that obtained in the quantum mode. Moreover, the temperature dependence of $\delta(\varphi_e)$ dip demonstrates that its width depends strongly on T. Therefore by analyzing the temperature dependence of $\delta(\varphi_e)$ one can easily distinguish between the quantum and classical modes.

In conclusion, we have analyzed the temperature dependence of the imaginary part of the impedance for three-junction loop–tank-circuit arrangement in the quantum and classical modes. We argued that the temperature dependence of the impedance for these modes is quite different, and they can therefore easily be distinguished experimentally.

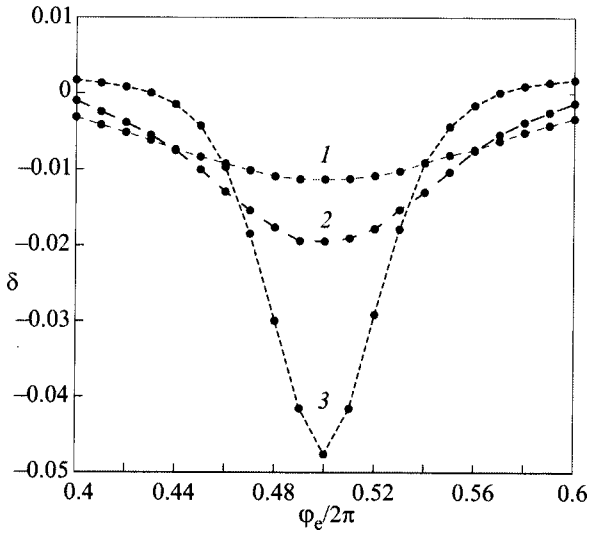

FIG. 8. The phase shift $\delta(\varphi_e)$ in the classical mode. $\alpha=0.8$ and $D=0.3$ (*1*), $D=0.2$ (*2*), $D=0.1$ (*3*).

APPENDIX A: QUANTUM MODE OF A FLUX QUBIT

Since the tunnel splitting in flux qubit is much smaller than the difference between upper energy levels, qubits are effectively two-level quantum systems. In the two level approximation a flux qubit can be described by the pseudo-spin Hamiltonian

$$H(t)=-\Delta\sigma_x-\varepsilon\sigma_z, \tag{A1}$$

where σ_x and σ_z are the Pauli matrices; Δ is the tunneling amplitude. The qubit bias is given by $\varepsilon=I_p\Phi_0 f_e$, where I_p is the magnitude of the qubit persistent current, and $f_e=\Phi_e/\Phi_0-1/2$. The stationary energy levels can be easily found from the Hamiltonian (A1):

$$E_{\pm}(\varepsilon)=\pm\sqrt{\varepsilon^2+\Delta^2}, \tag{A2}$$

and the average value of the qubit current at temperature T is:

$$I(\varepsilon) = \frac{\varepsilon I_p}{\sqrt{\varepsilon^2 + \Delta^2}} \tanh \frac{\sqrt{\varepsilon^2 + \Delta^2}}{kT}. \quad \text{(A3)}$$

Note that the dependence (A2) is valid within a narrow interval of Φ_e near $\Phi_e = \Phi_0/2$ where the potential U (13) is bistable.

[a)]Email: omelyanchouk@ilt.kharkov.ua

[1]A. Barone and G. Paterno, *Physics and Applications of the Josephson Effect*, Wiley, New York (1982).
[2]V. A. Khlus and I. O. Kulik, Sov. Tech. Phys. Lett. **20**, 283 (1975).
[3]L. D. Jackel, R. A. Buhrman, and W. W. Webb, Phys. Rev. B **10**, 2782 (1974).
[4]E. Il'ichev, V. Zakosarenko, V. Schultze, H.-G. Meyer, H. E. Hoenig, V. N. Glyantsev, and A. Golubov, Appl. Phys. Lett. **72**, 731 (1998).
[5]R. de Bruyn Ouboter and A. N. Omelyanchouk, Physica B **216**, 37 (1995).
[6]E. Il'ichev, V. Zakosarenko, R., P. J. IJsselsteijn, and V. Schultze, J. Low Temp. Phys. **106**, 503 (1997).
[7]E. Il'ichev, V. Zakosarenko, V. Schultze, H. E. Hoenig, H.-G. Meyer, K. O. Subke, H. Burkhard, and M. Schilling, Appl. Phys. Lett. **76**, 100 (2000).
[8]J. E. Mooij, T. P. Orlando, L. Levitov, L. Tian, C. H. van der Wal, and S. Lloyd, Science **285**, 1036 (1999).
[9]C. W. Gardiner, *Handbook of Stochastic Methods*, 2nd ed., Springer, Berlin (1990).
[10]E. Il'ichev, A. Yu. Smirnov, M. Grajcar, A. Izmalkov, D. Born, N. Oukhanski, Th. Wagner, H.-G. Meyer, W. Krech, and A. Zagoskin, Fiz. Nizk. Temp. **30**, 823 (2004) [Low Temp. Phys. **30**, 620 (2004)].
[11]S. N. Shevchenko, Eur. Phys. J. B **61**, 187 (2008).

This article was published in English in the original Russian journal. Reproduced here with stylistic changes by AIP.